

*Environmental Chemistry*

## USE OF A PARALLEL ARTIFICIAL MEMBRANE SYSTEM TO EVALUATE PASSIVE ABSORPTION AND ELIMINATION IN SMALL FISH

JUNG-HWAN KWON, LYNN E. KATZ, and HOWARD M. LILJESTRAND\*

Department of Civil, Architectural and Environmental Engineering, The University of Texas at Austin, 1 University Station C1786, Austin, Texas 78712-0273, USA

(Received 10 January 2006; Accepted 15 May 2006)

**Abstract**—A parallel artificial lipid membrane system was developed to mimic passive mass transfer of hydrophobic organic chemicals in fish. In this physical model system, a membrane filter-supported lipid bilayer separates two aqueous phases that represent the external and internal aqueous environments of fish. To predict bioconcentration kinetics in small fish with this system, literature absorption and elimination rates were analyzed with an allometric diffusion model to quantify the mass transfer resistances in the aqueous and lipid phases of fish. The effect of the aqueous phase mass transfer resistance was controlled by adjusting stirring intensity to mimic bioconcentration rates in small fish. Twenty-three simple aromatic hydrocarbons were chosen as model compounds for purposes of evaluation. For most of the selected chemicals, literature absorption/elimination rates fall into the range predicted from measured membrane permeabilities and elimination rates of the selected chemicals determined by the diffusion model system.

**Keywords**—Bioconcentration Artificial membranes Fish Diffusion

## INTRODUCTION

Bioconcentration of hydrophobic organic chemicals by fish from water has been modeled by employing physicochemical partitioning between water and lipid tissues and diffusion through a series of aqueous and lipid barriers [1–4]. Without active transport or metabolic transformation, uptake and elimination of hydrophobic organic chemicals are often evaluated by simple first-order rate expressions, assuming that a fish can be represented as a single compartment. In this sense, many abiotic devices are available for evaluating bioconcentration equilibrium or uptake/elimination rates of hydrophobic organic chemicals (e.g., [5–8]). Furthermore, this simplistic approach has been used to assess the toxicity of accumulative water pollutants as well as the time-averaged aqueous concentration [7,9].

More recently, a high-throughput parallel artificial membrane permeability assay has been developed to estimate human intestinal absorption of orally administered drugs [10–13]. This type of device also has potential for assessing bioconcentration in fish. The greatest advantage of the parallel artificial membrane permeability assay is that the microporous filter-supported bilayers have similar properties to actual biological membranes [14]. Measured permeability correlates well with percent absorption of orally administered drugs that passively permeate intestinal aqueous and lipid barriers [12,13]. This implies that the parallel artificial membrane permeability assay has the potential for evaluating uptake and elimination rates in fish, when uptake and elimination are governed by passive transcellular diffusion. Furthermore, this system allows easy access to both the external aqueous environment and the internal aqueous solution of a fish, thereby allowing the development of a monitoring system that combines passive transport processes to target sites and adverse toxic effects that occur at cellular/molecular levels. The first step is

to construct an artificial membrane system analogous to the membrane systems present in aquatic organisms with respect to absorption and elimination characteristics.

Thus, the goal of this research was to develop a parallel artificial membrane system that mimics passive mass transfer of hydrophobic organic chemicals in fish. The artificial membrane system developed was tuned to mimic bioconcentration rates in small fish by adjusting the mass transfer resistance in the aqueous phase. The characteristic length of the diffusion boundary layer in the artificial membrane system was determined from the permeability of weak organic acids under variable stirring intensity. After the optimal stirring intensity was determined for the desired diffusion characteristics, the absorption/elimination behavior of the artificial membrane system was evaluated with effective membrane permeabilities and elimination rates of 23 selected simple aromatic chemicals and compared with literature values of absorption and elimination rates for small fish.

## MATERIALS AND METHODS

*Chemicals*

Twenty-three simple aromatic chemicals—phenol, aniline, four nitroanilines (2-nitroaniline, 3-nitroaniline, 4-nitroaniline, and 2,4-dinitroaniline), six chloroanilines (2-chloroaniline, 3-chloroaniline, 4-chloroaniline, 2,4-dichloroaniline, 3,4-dichloroaniline, and 2,3,5,6-tetrachloroaniline), bromobenzene, and 10 chlorobenzenes (chlorobenzene, 1,3-dichlorobenzene, 1,4-dichlorobenzene, 1,2,3-trichlorobenzene, 1,2,4-trichlorobenzene, 1,3,5-trichlorobenzene, 1,2,3,4-tetrachlorobenzene, 1,2,4,5-tetrachlorobenzene, pentachlorobenzene, and hexachlorobenzene)—were chosen for evaluation of the bioconcentration rate parameters because they are stable and their uptake/elimination rates have been reported in the literature. Five organic acids—benzoic acid, 2,4-dinitrophenol, 2,4-dinitro-*o*-cresol, 2,4-dichlorophenol, and 2,4,6-trichlorophenol—were used to determine the aqueous diffusion layer thick-

\* To whom correspondence may be addressed (liljestrand@mail.utexas.edu).

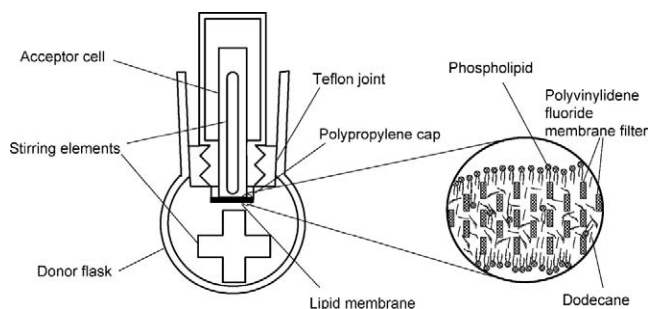


Fig. 1. Schematic of the artificial membrane permeation reactor with suggested microstructure of filter-supported lipid bilayers (reconstructed from Thompson et al. [14]).

ness. All of these chemicals were of high purity and obtained from Sigma-Aldrich (St. Louis, MO, USA), Fluka (Milwaukee, WI, USA), or Fischer Scientific (Pittsburgh, PA, USA). Acetonitrile and water were used as eluents for high-performance liquid chromatography (HPLC) analysis. *n*-Hexane was used for extraction of lipid membranes and as the solvent for gas chromatography (GC) analysis. Polyvinylidene fluoride membrane filters (0.1- $\mu\text{m}$  pore size, 125- $\mu\text{m}$  thickness) were purchased from Millipore (Billerica, MA, USA). Buffer solutions (30 mM) were prepared from phosphoric acid for pH 2.0 to 3.0, acetic acid for pH 3.8 to 5.6, potassium dihydrogen phosphate for pH 6.2 to 8.2, and anhydrous disodium tetraborate ( $\text{Na}_2\text{B}_4\text{O}_7$ ) for pH 8.5 to 10.0. The ionic strength of each buffer solution was adjusted to 154 mM with NaCl. The lipid phase in this study was dodecane containing 1% (w/w) of a phosphatidylcholine lipid mixture. Although lipid membrane permeation is more likely to be dominated by the dodecane, the lipid mixture comprised 25% didocosahexaenoylphosphatidylcholine (22:6, 22:6), 20% dioleoylphosphatidylcholine (18:1, 18:1), 15% stearyl docosahexaenoylphosphatidylcholine (18:0, 22:6), 10% dipalmytoylphosphatidylcholine (16:0, 16:0), and 30% cholesterol on the basis of the general fatty acid composition of fish gill [15,16]. Chloroform solutions of all phosphatidylcholines were purchased from Avanti Polar Lipids (Albaster, AL, USA).

#### Chemical analyses

For the determination of membrane permeability, aqueous samples of the donor and the acceptor cells of custom-made experimental reactors shown in Figure 1 were analyzed with a Waters 2690 HPLC system equipped with a Waters 996 PDA detector (Milford, MA, USA) on a C18 column (Waters Nova-Pak,  $3.9 \times 150$  mm) at 40°C. The HPLC flow rate was 1.5 ml/min, and the eluent was an isocratic composition of water and acetonitrile that varied depending on the polarity of the analyte mixture. The concentration of each compound was measured at its optimum absorption wavelength.

For the elimination experiments, concentrations of *n*-hexane extracts of lipid membranes were measured by GC-electron capture detector (ECD) with an HP6890 gas chromatographer (Hewlett-Packard, Palo Alto, CA, USA) equipped with a  $^{63}\text{Ni}$   $\mu\text{ECD}$ . Recoveries of all analytes ranged from approximately 85 to 110%. One microliter of extract was injected in a splitless mode onto a 30 m by 0.25 mm DB1701 column (J&W Scientific, Folsom, CA, USA) with a 0.25- $\mu\text{m}$  film thickness. Hydrogen was used as a carrier gas at a flow rate of 0.9 ml/min. Injector and detector temperatures were 250°C

and 280°C, respectively. Column temperature varied depending on the analyte mixture.

#### Diffusion mass transfer model

A diffusion mass transfer model proposed by Gobas et al. [1] was used to model bioconcentration and to evaluate the parallel artificial membrane system. In this model, molecules pass through a series of aqueous and lipid membrane barriers during transport between the ambient water and the storage compartments. This model is consistent with the hypothesis that the main uptake route of hydrophobic organic chemicals is passive diffusion through fish gill made of multiple layers of lipid membrane lamellas and water [17]. For a simple two-compartment model with first-order rates, the bioconcentration model can be expressed as

$$\frac{dC_f}{dt} = k_a C_w - k_e C_f \quad (1)$$

in which  $C_w$  and  $C_f$  are the concentrations of the pollutant in water ( $\mu\text{g}/\text{cm}^3$ ) and fish ( $\mu\text{g}/\text{g}$ ),  $k_a$  is a first-order absorption rate constant ( $\text{cm}^3/\text{g}\cdot\text{h}$ ), and  $k_e$  is a first-order elimination rate constant ( $\text{h}^{-1}$ ). The two rate parameters,  $k_a$  and  $k_e$ , can be determined by aqueous and membrane resistances as in Equation 2 [1,3],

$$k_a = P \frac{A}{W} = \frac{1}{\frac{\delta_w}{D_w} + \frac{\delta_m}{K_m D_m}} \frac{A}{W} \quad (2)$$

$$k_e = \frac{1}{\frac{\delta_w}{D_w} + \frac{\delta_m}{K_m D_m}} \frac{1}{(1 - \alpha) + \alpha K_m} \frac{A}{W} \quad (3)$$

where  $P$  is overall permeability (cm/h);  $\delta_w$  and  $\delta_m$  are the thickness of aqueous and membrane diffusion films (cm), respectively;  $D_w$  and  $D_m$  are diffusion coefficients ( $\text{cm}^2/\text{h}$ ) in water and in the membrane, respectively;  $\alpha$  is the lipid content;  $K_m$  is the lipid membrane-water partition coefficient;  $A$  is interface area ( $\text{cm}^2$ ); and  $W$  is fish weight (g).

#### Evaluation of the literature bioconcentration rate constants

Twenty-three simple aromatic organic chemicals were selected for the evaluation of a diffusion mass transfer model and the performance of the artificial membrane system. Their bioconcentration mass transfer coefficients (often referred to as uptake and elimination rate constants) have been reported for small fish (0.1–5.0 g) by many authors [3,18–27]. Data on small fish were chosen to avoid significant allometric effects other than changes in surface to volume ratio. These uptake and elimination rate constants were normalized to that of a standard 1-g fish according to an allometric relationship (Eqn. 4) [28],

$$\frac{A}{W} = (5.59 \pm 3.16 \text{ cm}^2 \text{ g}^{-0.77}) W^{-0.23} \quad (4)$$

where  $A$  is surface area of permeation ( $\text{cm}^2$ ) and  $W$  is weight of fish (g). Normalized absorption/elimination rates ( $k_{a,\text{norm}}/k_{e,\text{norm}}$ ) can be calculated by substituting Equation 4 into Equation 2 and assuming that permeability ( $P$ ) does not change significantly for the selected fish size.

$$k_{a,\text{norm}}(\text{or } k_{e,\text{norm}}) = k_a(\text{or } k_e) W^{0.23} \quad (5)$$

Aqueous and membrane resistances were calculated from the diffusion mass transfer model described in Equation 2 with

normalized uptake rate constants of the selected chemicals by a least square regression with  $K_{OW}$  as a surrogate for the membrane–water partition coefficient ( $K_m$ ) in Equation 2. Median values of  $k_{a, norm}$  were chosen when multiple data were available for a chemical.

### Membrane permeability

Permeability experiments were carried out at 25°C in a custom-made reactor (Fig. 1). A 0.35-ml shell insert and a 5-ml volumetric flask were used as acceptor and donor cells, respectively. These two cells were separated by two sheets of polyvinylidene fluoride membrane filter (0.1  $\mu\text{m}$  pore size, 125  $\mu\text{m}$  thickness, Millipore) thermally attached to a polypropylene cap. The polypropylene surfaces were wrapped with Teflon® tape to minimize surface contact. Aqueous buffer solution was filled in the acceptor cell. As soon as 5  $\mu\text{l}$  of the dodecane/lipid solution described above was applied to the membrane filter, the acceptor cell was closed and attached to the donor cell that had been pre-filled with buffer containing the chemical species. The reactor was stirred with a VP710C1 tumble stirrer (V&P Scientific, San Diego, CA, USA) to maximize vertical mixing. Incubation time varied from 10 min to 30 h, depending on the chemical's permeability and the stirring intensity. After incubation, the reactor was disassembled, and the solutions in both the donor and acceptor cells were analyzed by HPLC. Membrane resistance was measured with an HP 3466A digital multimeter (Hewlett-Packard) with custom-made copper electrodes to ensure that membrane permeation was not due to unfilled pores or gaps in the membrane cap. Data were accepted when the electrical resistance across the membrane was greater than 50 k $\Omega$ .

The change in concentration of the acceptor solution with respect to time can be expressed as a simple differential equation and an effective permeability,  $P_{eff}$  (cm/h).

$$\frac{dC_A}{dt} = \frac{P_{eff}A}{V_A}(C_D - C_A) \quad (6)$$

The  $C_A$  and  $C_D$  are the concentrations in the acceptor and the donor cells (mg/L), respectively,  $A$  is the surface area of membrane permeation (0.124  $\text{cm}^2$ ),  $V_A$  is the volume of the acceptor cell ( $\text{cm}^3$ ), and  $t$  is the incubation time (s). The  $P_{eff}$  is obtained by solving Equation 6, assuming negligible membrane retention,

$$P_{eff} = -\frac{V_D V_A}{(V_D + V_A)A t} \ln\left(1 - \frac{C_A}{C_{eq}^*}\right) \quad (7)$$

where  $C_{eq}^*$  is the theoretical equilibrium concentration that represents the concentration in donor and acceptor cells after equilibrium is reached, calculated with a mass balance equation that includes membrane retention. For more hydrophobic chemicals having membrane retention greater than 15% of the total mass, Equation 8 was used instead, assuming that membrane holding occurs within a short loading time,  $\tau_{SS}$  [29].

$$P_{eff} = -\frac{V_D V_A}{(V_D + V_A)A(t - \tau_{SS})} \ln\left(1 - \frac{C_A}{C_{eq}^*}\right) \quad (8)$$

The  $P_{eff}$ ,  $\tau_{SS}$ , and  $C_{eq}^*$  were estimated as best fit parameters by plotting  $C_A$  versus  $t$ . Nonlinear regression analyses were performed by SPSS for Windows (Ver 12.0; SPSS, Chicago, IL, USA).

### Determining the thickness of diffusion layers

In the model artificial system, the overall resistance is assumed to be a sum of the artificial lipid membrane resistance and aqueous diffusion layer resistances on both sides of the membrane. Thus, the effective permeability, the inverse of the overall resistance, is written as in Equation 9,

$$\frac{1}{P_{eff}} = \frac{1}{P_{aq}} + \frac{1}{P_m} \quad (9)$$

where  $P_{aq}$  is the permeability of the aqueous diffusion layer including both sides (cm/h), and  $P_m$  is the permeability of the artificial lipid membrane (cm/h).

Because the artificial membrane is not permeable to ionized species, the membrane permeability,  $P_m$ , depends on the pH of the solution for an ionizable chemical. For a monoprotic weak acid,  $P_m$  is obtained by multiplying intrinsic membrane permeability,  $P_o$ , and the fraction of the un-ionized species [30].

$$P_m = \frac{P_o}{10^{(\text{pH} - \text{p}K_a)} + 1} \quad (10)$$

$$\frac{1}{P_{eff}} = \frac{1}{P_{aq}} + \frac{10^{(\text{pH} - \text{p}K_a)} + 1}{P_o} \quad (11)$$

Both  $P_{aq}$  and  $P_o$  can be calculated by plotting  $P_{eff}$  versus pH when the  $\text{p}K_a$  of the acid is known. The  $P_{aq}$  and  $P_o$  were determined for the selected organic acids at different stirring intensities with a nonlinear least square regression. The  $\text{p}K_a$  values obtained from the literature were corrected for the ionic strength of the solution,  $I$ , with the Davies equation for a monoprotic acid (Eqn. 12) [31],

$$\text{p}K'_a = \text{p}K_a - \left[ \frac{A\sqrt{I}}{(1 + I)} - 0.2I \right] \quad (12)$$

where  $\text{p}K'_a$  is the negative log of the ionic strength–corrected mixed acidity constant,  $\text{p}K_a$  is the negative log of the infinite dilution equilibrium constant, and  $A$  is a constant that has a value of 0.5 at 25°C.

The thickness of the aqueous diffusion layer is calculated from the aqueous permeability and calculated diffusion coefficient with the use of molecular mass ( $D_{aq}$ ,  $\text{cm}^2/\text{h}$ ) [32], as in Equations 13 and 14,

$$\delta_{aq} = \frac{D_{aq}}{P_{aq}} \quad (13)$$

$$D_{aq} (\text{cm}^2 \text{h}^{-1}) = \frac{0.972}{M^{0.71}} \quad (14)$$

where  $\delta_{aq}$  is the thickness of the aqueous diffusion layer (cm),  $D_{aq}$  is the aqueous diffusion coefficient of the acid ( $\text{cm}^2/\text{h}$ ), and  $M$  is the molecular mass of a solute (g/mol).

### Elimination rate constants

Elimination rate constants from the artificial membrane were measured for the 13 most hydrophobic chemicals. The reactor used for the permeability experiments was modified to allow the aqueous buffer solution (pH 7.4,  $I = 154$  mM) to flow through the donor cell. The experimental procedure was the same as that used in the permeability measurement, except that the 5- $\mu\text{l}$  dodecane/lipid mixture applied to the polyvinylidene fluoride membrane also contained the chemical species. The flow rate of approximately 1 ml/min was sufficient

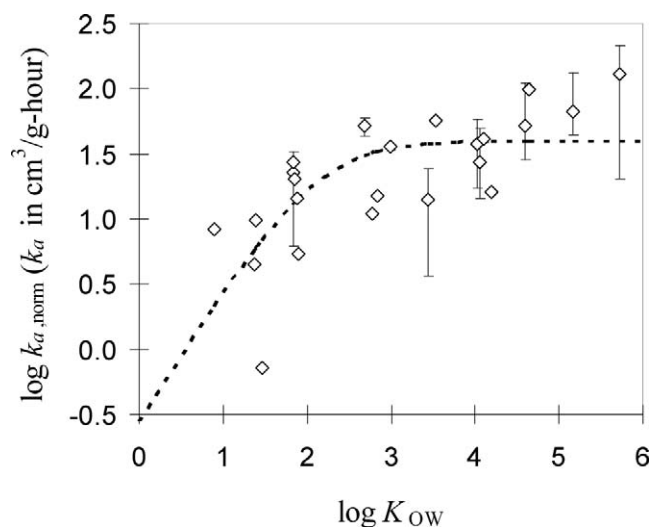


Fig. 2. Log  $k_{a, \text{norm}}$  versus log  $K_{\text{OW}}$  for 23 selected simple aromatic chemicals. Broken line indicates Equation 17. Median values of the uptake rate constant were chosen when there are multiple values for one chemical. The error bar denotes the range of literature values for one chemical when multiple values are available.

to ensure that the aqueous concentration in the donor cell was much smaller than the equilibrium concentration and that re-absorption from the aqueous phase was negligible. After incubation, the polyvinylidene fluoride membrane cap was disassembled and placed into a 10-ml vial containing 5 ml of *n*-hexane. After shaking for 30 min, the species concentration in the *n*-hexane extract was measured with a GC-electron capture detector. The elimination rate constant was calculated with a first-order rate expression (Eqn. 15),

$$C_M(t) = C_{M,0} \exp(-k_e t) \quad (15)$$

where  $C_M(t)$  is the membrane concentration after time  $t$  (mg/L),  $C_{M,0}$  is the initial membrane concentration (mg/L),  $k_e$  is the elimination rate constant ( $\text{h}^{-1}$ ), and  $t$  is incubation time (h). The  $k_e$  was calculated from regression of the linear form in Equation 16.

$$\ln \left[ \frac{C_M(t)}{C_{M,0}} \right] = -k_e t \quad (16)$$

## RESULTS

### Evaluation of literature data

Figure 2 shows the relationship between log  $k_{a, \text{norm}}$  and log  $K_{\text{OW}}$ . Consistent with the diffusion model, uptake rates increased with increasing hydrophobicity for log  $K_{\text{OW}} < 2$  and then approached a plateau for more hydrophobic chemicals. Best fit parameters were obtained by least square regression (Eqn. 17).

$$k_{a, \text{norm}} (\text{cm}^3 \text{g}^{-1} \text{h}) = \frac{K_{\text{OW}}}{3.570 + 0.0252K_{\text{OW}}} \quad (17)$$

From Equations 2 and 4, the corresponding membrane resistance ( $\delta_m/D_m$ ) and aqueous resistance ( $\delta_w/D_w$ ) were determined to be 20.0 h/cm and 0.141 h/cm, respectively. The corresponding  $\delta_w$  is about 27  $\mu\text{m}$  for a typical water pollutant (molecular mass of 250 g/mol) with  $D_w = 0.019 \text{ cm}^2/\text{h}$  calculated from Equation 13. Diffusion thickness of the membrane phase could not be determined because  $D_m$  was unknown. Aqueous phase resistance was also calculated from the

average uptake rate constant of the most hydrophobic chemicals (i.e., chemicals with literature lipid-normalized bioconcentration factors  $>10^{4.5}$ ) for which membrane resistance was assumed to be negligible. The  $\delta_w/D_w$  was calculated to be 0.114 h/cm, and the corresponding  $\delta_w$  was 22  $\mu\text{m}$ . The slight decrease in  $\delta_w$  is due to a slight increase of  $k_{a, \text{norm}}$  at log  $K_{\text{OW}} > 3$  (Fig. 2). However, this value is not significantly different from that value obtained by regression, which indicated that membrane resistance equals the aqueous resistance when log  $K_{\text{OW}}$  of the chemical is 2.15.

### Determination of the thickness of the aqueous diffusion layer

Figure 3 presents the changes in  $P_{\text{eff}}$  of five standard organic acids as a function of pH. The  $P_{\text{eff}}$  is proportional to the fraction of the un-ionized species in the system, showing that  $P_{\text{eff}}$  did not change with increasing pH at values less than the  $\text{p}K_a$  and decreased with increasing pH with a slope of  $-1$  for  $\text{pH} > \text{p}K_a$ . The  $P_{\text{eff}}$ , depicted by solid lines, increased with increasing stirring speed unless it was limited by membrane diffusion, whereas membrane permeability ( $P_m$ ), described in dashed lines, did not change regardless of the stirring speed. The  $P_{\text{eff}}$  for benzoic acid and 2,4-dinitrophenol was close to  $P_m$  at 40 rpm, indicating that the overall permeability is limited by membrane diffusion at stirring speeds greater than 40 rpm. Thus, the corresponding thickness of the aqueous diffusion layer ( $\delta_w$ ) could not be calculated when the resistance to permeation of solutes was dominated by membrane diffusion. For the other three acids,  $P_{\text{eff}}$  is at least one order of magnitude lower than  $P_m$ , indicating that the aqueous resistance dominates. Thus,  $\delta_w$  was calculated for all stirring speeds for these acids. The  $\delta_w$  values were between 1,900 and 5,000  $\mu\text{m}$  for unstirred experiments, between 58 and 92  $\mu\text{m}$  at 40 rpm, between 18 and 26  $\mu\text{m}$  at 300 rpm, and between 14 and 17  $\mu\text{m}$  at 800 rpm. For permeability assays of the selected chemicals, 300 rpm was chosen because  $\delta_w$  was close to that obtained in the previous section and the reactor was more stable at 300 rpm than at 800 rpm.

### Artificial membrane permeability

The artificial membrane permeabilities ( $P_{\text{eff}}$ ) of phenol, the 10 anilines, bromobenzene, and the three chlorobenzenes are presented in Table 1. The  $P_{\text{eff}}$  was calculated from measured aqueous concentrations in the donor and acceptor cells of the less hydrophobic chemicals, because their membrane retention was not significant ( $<15\%$  by mass). The  $P_{\text{eff}}$  was calculated from data collected in triplicate reactors for at least three different incubation times. Because  $P_{\text{eff}}$  was not affected significantly by incubation time for these chemicals, all values were averaged and the standard deviation was calculated from all data. Equation 8 was used to obtain  $P_{\text{eff}}$  for the more hydrophobic chemicals, chlorobenzene, bromobenzene, 1,3-dichlorobenzene, and 1,4-dichlorobenzene. Their membrane retentions ranged from 47 to 83% by mass (Appendix). Standard error in  $P_{\text{eff}}$  from the nonlinear regression was used instead of the standard deviation (Table 1). The  $P_{\text{eff}}$  generally increased with increasing chemical hydrophobicity ( $K_{\text{OW}}$ ) and approached an upper limit value of approximately 7 cm/h, a value limited by aqueous diffusion resistance (Fig. 3).

### Elimination rate constant

Elimination rate constants of the 13 chemicals from the artificial membrane (Table 1) were calculated from membrane



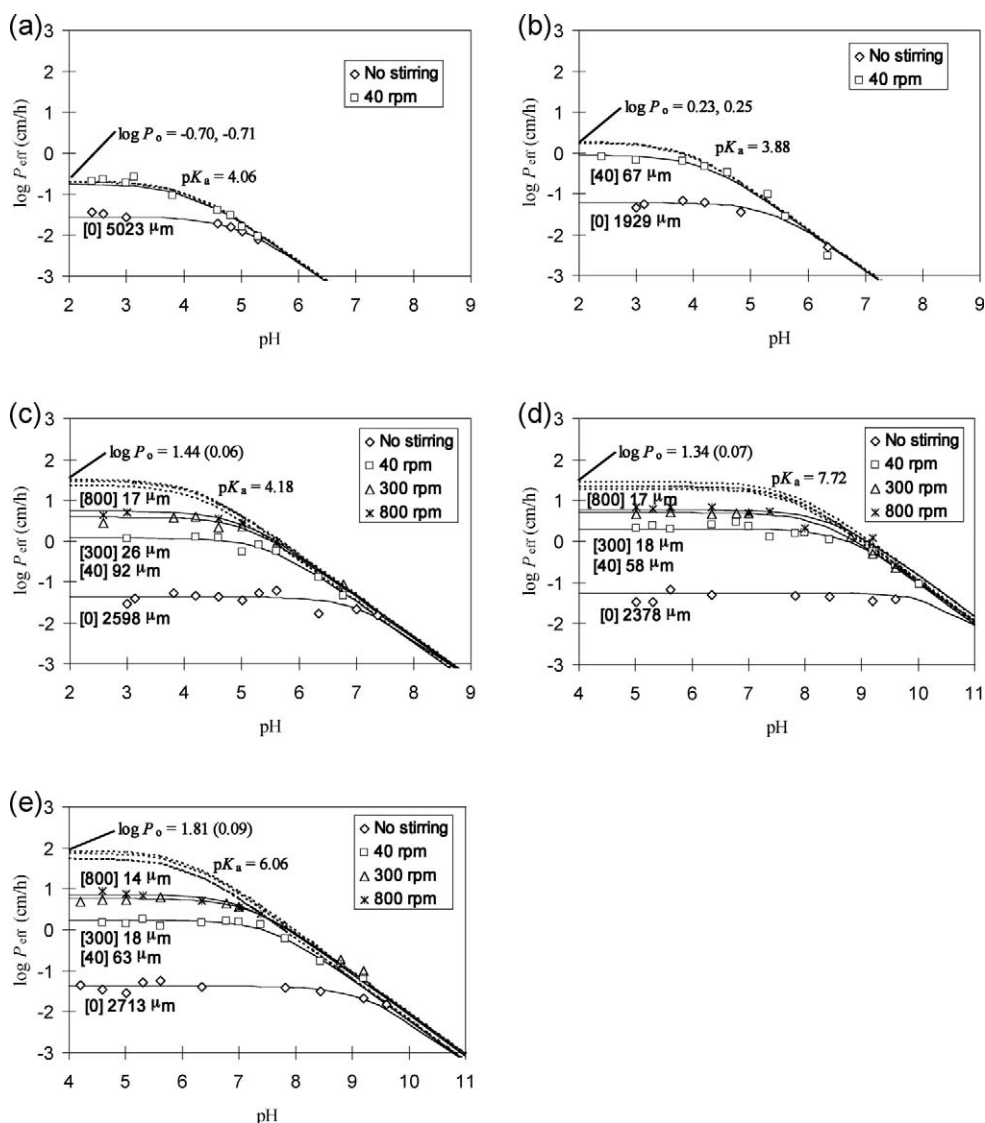


Fig. 3. Log permeability (cm/h) versus pH plots for five standard acids: (a) benzoic acid (BZA), (b) 2,4-dinitrophenol (DNP), (c) 2,4-dinitro-*o*-cresol (DNOC), (d) 2,4-dichlorophenol (DCP), and (e) 2,4,6-trichlorophenol (TCP). Solid curves represent the best fit of measured  $\log P_{\text{eff}}$  versus pH according to Equation 11. The estimated thickness ( $\mu\text{m}$ ) of the aqueous diffusion layer is indicated with the corresponding stirring speed in square bracket. The dashed curves are the calculated intrinsic permeability curves from Equation 10. The mean values of  $\log P_o$  are indicated in the frames along with the estimated standard deviation in parentheses.

concentrations measured at different times with the linear regression  $\ln(C_M(t)/C_{M,0})$  versus  $t$  in Equation 16. Corresponding half-lives of the chemicals in the membrane ranged from 10 min for the dichloroanilines to 5 d for hexachlorobenzene. The correlation coefficients,  $r^2$ , of the regression were greater than 0.9 for all the chemicals except hexachlorobenzene (Appendix). Smaller correlation coefficients for hexachlorobenzene could be a result of the relatively short incubation time.

## DISCUSSION

### Diffusion mass transfer model

According to the diffusion model described above, the uptake rate constant ( $\log k_a$ ) should increase with increasing membrane/water partition coefficient ( $\log K_m$ ), with a slope of unity for less hydrophobic chemicals and reaching an upper limit as aqueous resistance dominates. Although some of the observed results deviate from that expected (Fig. 2), the relationship between normalized uptake rate constants ( $k_{a,\text{norm}}$ ) and  $K_{\text{OW}}$  as a surrogate for  $K_m$  shows the general trend predicted

by the diffusion mass transfer model. Quality of fit is better for the more hydrophobic chemicals, and conversely, less hydrophobic chemicals deviate more from the relationship. This tendency suggests that transport of less hydrophobic chemicals is not solely due to passive permeation processes, as assumed in the diffusion model.

Previous studies showed that uptake rate constants increase with  $\log K_{\text{OW}}$  and are independent of  $\log K_{\text{OW}}$  for  $\log K_{\text{OW}}$  between 3 and 6 [1,4,33]. The break point for dependence on  $\log K_{\text{OW}}$  was estimated in the literature to be  $\log K_{\text{OW}} \approx 3$  [1,33], whereas the regression results in this study indicated it to be less than 3, perhaps because of the greater deviation from the suggested relationship, especially for less hydrophobic chemicals. Hawker and Connell [33] developed an empirical curvilinear relationship between  $k_a$  and  $K_{\text{OW}}$ , mostly with the use of chlorobenzenes (Eqn. 18).

$$k_a = \frac{0.048K_{\text{OW}}}{0.00142K_{\text{OW}} + 12.01} \quad (18)$$

Table 1. Log  $K_{OW}$ , artificial membrane permeabilities ( $P_{eff}$ ) and elimination rate constants ( $k_e$ ), and literature absorption ( $k_{a,norm}$ ) and elimination rate ( $k_{e,norm}$ ) constants for selected chemicals

Chemicals	Experimental values			Median literature values <sup>b</sup>		
	Log $K_{OW}$ <sup>a</sup>	$P_{eff}$ (cm/h)	$k_e$ (h <sup>-1</sup> )	$k_{a,norm}$ (cm <sup>3</sup> /g·h)	$k_{e,norm}$ (h <sup>-1</sup> )	Reference
Phenol	1.46	0.15 ± 0.02	—	0.72	0.040	[22]
Aniline	0.90	1.05 ± 0.18	—	8.29	4.06	[21,23]
2-Nitroaniline	1.85	0.94 ± 0.24	—	20.3	2.50	[21]
3-Nitroaniline	1.37	0.26 ± 0.05	—	4.47	0.54	[21]
4-Nitroaniline	1.39	0.083 ± 0.008	—	9.78	2.20	[21]
2,4-Dinitroaniline	1.84	0.078 ± 0.006	—	27.4	2.12	[21]
2-Chloroaniline	1.90	4.93 ± 0.46	—	5.38	0.35	[21]
3-Chloroaniline	1.88	3.02 ± 0.33	—	14.5	1.29	[21]
4-Chloroaniline	1.83	2.67 ± 0.30	—	22.5	3.06	[21,23,25]
2,4-Dichloroaniline	2.78	6.50 ± 1.03	9.0	10.9	0.12	[21]
3,4-Dichloroaniline	2.69	3.70 ± 0.93	12.7	51.4	1.59	[21,22]
2,3,5,6-Tetrachloroaniline	4.10	—	0.14	41.6	0.14	[24]
Monochlorobenzene	2.84	6.82 ± 1.79 <sup>c</sup>	—	15.2	0.30	[27]
Bromobenzene	2.99	5.60 ± 1.90 <sup>c</sup>	0.90	36.1	0.21	[27]
1,3-Dichlorobenzene	3.53	7.95 ± 5.60 <sup>c</sup>	0.26	57.3	0.086	[27]
1,4-Dichlorobenzene	3.44	5.92 ± 3.32 <sup>c</sup>	0.26	14.0	0.38	[18,20]
1,2,3-Trichlorobenzene	4.05	—	0.059	27.2	0.0095	[3,18]
1,2,4-Trichlorobenzene	4.02	—	0.087	37.9	0.023	[20,26]
1,3,5-Trichlorobenzene	4.19	—	0.11	16.1	0.28	[18]
1,2,3,4-Tetrachlorobenzene	4.60	—	0.024	51.8	0.0098	[3,19]
1,2,4,5-Tetrachlorobenzene	4.64	—	0.031	98.7	0.017	[20]
Pentachlorobenzene	5.17	—	0.012	66.1	0.0114	[3,18,19]
Hexachlorobenzene	5.73	—	0.0054	129.2	0.0004	[3,18]

<sup>a</sup> Log  $K_{OW}$  values are suggested experimental values from KOWWIN program [36].

<sup>b</sup> Median values are used when multiple data are available for a chemical.

<sup>c</sup> Standard error obtained from nonlinear regression analyses.

According to their relationship, the aqueous phase resistance equals the membrane phase resistance at  $\log K_{OW} = 3.8$ . Hawker and Connell [33] did not analyze many compounds with lower hydrophobicity as needed to verify the linearly increasing unit slope. Thus, membrane resistance was determined from the slight variation in  $k_a$  for moderately hydrophobic chemicals. Although their ratio of aqueous resistance to membrane resistance shown in Equation 18 is different from that in this study (Eqn. 17), their maximum value of  $k_a$  (33.8 cm<sup>3</sup>/g·h) is very close to that obtained in this study, 39.7 cm<sup>3</sup>/g·h. This suggests that the mass transfer of highly hydrophobic chemicals is limited by aqueous diffusion.

#### Determination of the thickness of the aqueous diffusion layer

As proposed in previous research, most diffusion resistance for uptake of a chemical occurs in the fish gill [17]. Thus, the net aqueous diffusion layer for bioconcentration would be composed of an external aqueous film, interlamellar aqueous layer, mucous layers, etc. The distance between two gill lamellae is approximately 20  $\mu$ m for a 1-g fish [3,34]. From this value, Sijm and van der Linde [3] assumed that the aqueous diffusion path length is 10% of the interlamellar distance, and the viscosity of the solution is 10 times that of pure water. The aqueous phase resistance with the use of their assumption was equivalent to that for 20  $\mu$ m of pure water [3]. In terms of mass transfer resistances, the thickness of the aqueous diffusion layer from the previous studies was consistent with 22 to 27  $\mu$ m of pure water for a 1-g fish analyzed from Figure 2. Thus, stirring intensity was optimized at 300 rpm to obtain a  $\delta_w$  of  $20.7 \pm 4.6$   $\mu$ m calculated from the  $pK_a$  flux method with three acids: 2,4-dinitro-*o*-cresol, 2,4-dichlorophenol, and 2,4,6-trichlorophenol.

The thickness of the membrane phase in the system was about 300  $\mu$ m. With this membrane thickness, membrane permeation of less hydrophobic acids, benzoic acid and 2,4-dinitrophenol with  $\log K_{OW}$  values less than 2.0, were limited by membrane diffusion, whereas more hydrophobic acids, with  $\log K_{OW}$  greater than 2.0, were limited by aqueous diffusion at 300 rpm (Fig. 3). These results are consistent with the critical  $\log K_{OW}$  value obtained from Figure 2.

#### Comparison of uptake/elimination rate constants in fish with analogous parameters in the artificial membrane system

Artificial membrane permeability obtained either from Equation 7 or 8 could be related to the normalized absorption rate constant ( $k_{a,norm}$ ) from the literature. Although diffusion resistances in both aqueous and membrane phases are affected by fish size, allometric effects on mass transfer resistances could be neglected when rate constants are obtained from a relatively narrow range of fish sizes, 0.1 to 5 g. Fish permeability ( $P$ ) in Equation 2 should be comparable to the effective permeability obtained from the artificial membrane system if the two systems are not significantly different in terms of partitioning. Thus,  $k_{a,norm}$  values are directly related to artificial membrane permeability ( $P_{eff}$ ) from Equation 2 assuming  $P_{eff} \approx P$ . By taking logarithms of both sides of Equation 2 and using the surface to weight ratio of a 1-g fish ( $A/W = 5.59 \pm 3.16$  cm<sup>2</sup>/g) [28], Equation 19 is obtained.

$$\log k_{a,norm} = \log P_{eff} + \log(5.59 \pm 3.16) \quad (19)$$

Figure 4 represents the relationship between  $\log k_{a,norm}$  and  $\log P_{eff}$  obtained from the artificial membrane system, with the solid line representing Equation 19 and dashed lines indicating one standard deviation range of  $A/W$ . Seven chemicals fall

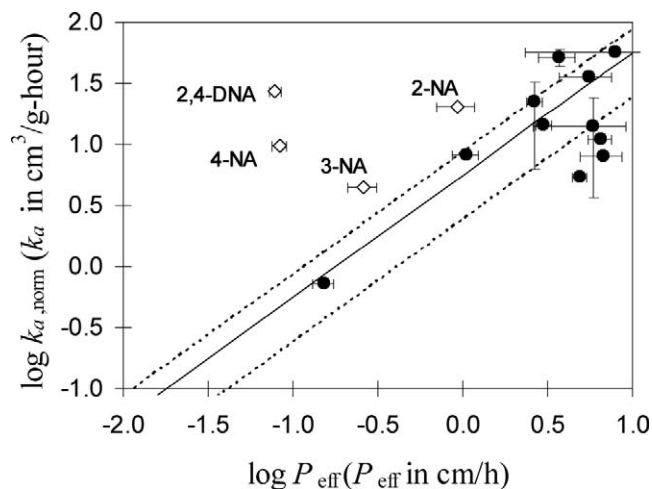


Fig. 4. Relationship between normalized literature absorption rate constants ( $k_{a, \text{norm}}$ ) and the artificial membrane permeability ( $P_{\text{eff}}$ ). Solid line indicates the theoretical relationship shown in Equation 19. Dashed lines indicate one standard deviation of surface to weight ratio. Vertical error bars denote the range of literature values when multiple data are available for one chemical. Horizontal error bars denote standard deviation or standard error from nonlinear regression.

within one standard deviation range of Equation 19, and the other chemicals were close to that theoretically expected, except for the nitroanilines. All nitroanilines are above Equation 19, indicating that the uptake rate of these chemicals in fish is much faster than expected on the basis of the artificial membrane permeability. Substitution of the nitro group enhances delocalization of  $\pi$  electrons in the benzene ring and stabilizes the conjugate base (neutral anilines). The permanent dipole moment (in Debye units [D]) of aniline (1.53 D) increases significantly by substitution of the nitro group. Dipole moments of 2-nitroaniline and 4-nitroaniline are 4.26 and 6.12 D, respectively [35]. Thus, the extremely low permeability of 2,4-dinitroaniline and 4-nitroaniline could be because of their strong dipole moments. In spite of their electrical properties, absorption rate constants of nitroanilines are similar to those of aniline and chloroanilines [21]. Relatively high absorption rate constants by fish indicate that uptake of nitroanilines by fish might not be described by passive diffusion across a series of biological barriers. Contributions of other uptake mechanisms for less hydrophobic chemicals would increase  $k_{a, \text{norm}}$  more than expected from the passive diffusion model. This also makes it difficult to fit less hydrophobic chemicals in the linear region of Figure 2.

In the diffusion mass transfer model, the elimination rate constant can be obtained from permeability ( $P_{\text{eff}}$ ), the membrane/water partition coefficient ( $K_m$ ), and a size-related factor ( $A/W$ ). Because elimination of the chosen hydrophobic chemicals are limited by aqueous diffusion, elimination rate constants from the artificial membrane ( $k_e$ ) should be related to that from fish, assuming that the artificial membrane and fish have the same  $K_m$  for a chemical. Thus, a normalized elimination rate constant from fish ( $k_{e, \text{norm}}$ ) can be expressed as Equation 20.

$$k_{e, \text{norm}} = \frac{(A/W)_{\text{fish}} \delta_{w, \text{AM}}}{(A/W)_{\text{AM}} \delta_{w, \text{fish}}} k_{e, \text{AM}} \quad (20)$$

Although the donor side thickness of the aqueous diffusion film could not be separated from the total thickness of the aqueous diffusion film by the  $pK_a$  flux method, it is thought

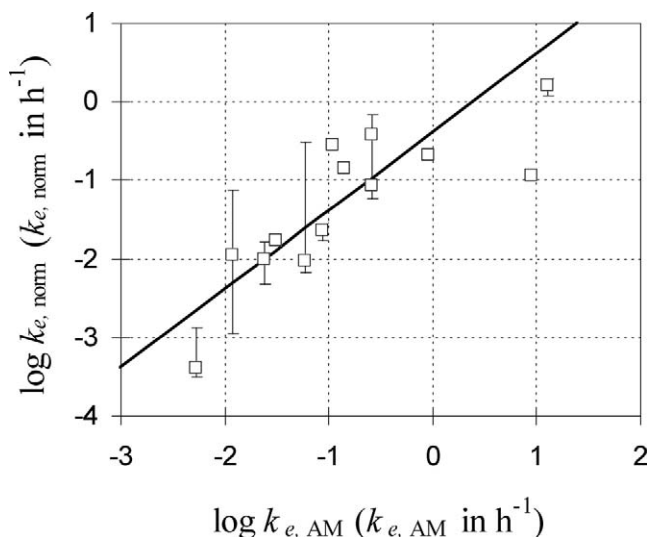


Fig. 5. Relationship between normalized literature elimination rate constants ( $\log k_{e, \text{norm}}$ ) and the artificial membrane elimination rate constant ( $\log k_{e, \text{AM}}$ ). Solid line indicates the theoretical relationship shown in Equation 21. Vertical error bars denote the range of literature values when multiple data are available for one chemical.

to be approximately 30 to 50% of the total thickness of the aqueous diffusion film. Estimates were approximately 9 to 11  $\mu\text{m}$  for bromobenzene, 1,3-dichlorobenzene, and 1,4-dichlorobenzene with the changes in concentration at the donor side and assuming that the absorption rate is solely limited by aqueous diffusion (Appendix). The outer surface area of the artificial membrane system was approximately 0.40  $\text{cm}^2$ , and the applied volume of the dodecane/lipid phase was 5  $\mu\text{l}$  (3.78 mg). If a typical small fish contains 5% lipid content, the corresponding weight would be approximately 0.076 g, and the value of  $(A/W)_{\text{AM}}$  would be 5.3  $\text{cm}^2/\text{g}$ . Therefore,  $k_{e, \text{norm}}$  is related to  $k_{e, \text{AM}}$  (Eqn. 21).

$$\log k_{e, \text{norm}} = \log k_{e, \text{AM}} - 0.4 \quad (21)$$

Figure 5 represents the relationship between  $\log k_{e, \text{norm}}$  and  $\log k_{e, \text{AM}}$ , with the solid line representing Equation 21. Deviations from the expected values are within 0.5 log units for most chemicals and at least within one order of magnitude for all chemicals except 2,4-dichloroaniline.  $\log k_{e, \text{norm}}$  of 2,4-dichloroaniline was extremely small compared with other structurally similar compounds [21]. The extraordinarily slow elimination rate of 2,4-dichloroaniline could not be explained by passive diffusion processes.

#### Potential application of this study

The parallel artificial membrane system developed in this study showed great potential for mimicking passive uptake and elimination processes in aquatic animals. This system has great applicability because it allows easy access to both aqueous solution sides of the membrane that correspond to the external aqueous environment and the internal aqueous solution in fish. More reliable risk prediction would be possible, especially for nonnarcotic pollutants, if highly sensitive chemical or biological sensors were placed in the acceptor phase of this parallel membrane system to evaluate specific toxicity. A combined system can emulate transport processes to target sites via passive diffusion and adverse toxic effects at the cellular and molecular levels.

## REFERENCES

- Gobas FAPC, Opperhuizen A, Hutzinger O. 1986. Bioconcentration of hydrophobic chemicals in fish: Relationship with membrane permeation. *Environ Toxicol Chem* 5:637–646.
- Barber MC, Suárez LA, Lassiter RR. 1988. Modeling bioconcentration of nonpolar organic pollutants by fish. *Environ Toxicol Chem* 7:545–558.
- Sijm DTHM, van der Linde A. 1995. Size-dependent bioconcentration kinetics of hydrophobic organic chemicals in fish based on diffusive mass transfer and allometric relationships. *Environ Sci Technol* 29:2769–2777.
- Chaisuksant Y, Yu Q, Connell DW. 1997. Bioconcentration of bromo- and chlorobenzenes by fish (*Gambusia affinis*). *Water Res* 31:61–68.
- Huckins JN, Tubergen MW, Manuweera GK. 1990. Semipermeable membrane devices containing model lipid: A new approach to monitoring the bioavailability of lipophilic contaminants and estimating their bioconcentration potential. *Chemosphere* 20:533–552.
- Huckins JN, Manuweera GK, Petty JD, Mackay D, Lebo J. 1993. A lipid-containing semipermeable membrane device for monitoring organic contaminants in water. *Environ Sci Technol* 27:2489–2496.
- Verbruggen EMJ, Vaes WHJ, Parkerton TF, Hermens JLM. 2000. Polyacrylate-coated SPME fibers as a tool to simulate body residues and target concentrations of complex organic mixtures for estimation of baseline toxicity. *Environ Sci Technol* 34:324–331.
- Verweij F, Booij K, Satumalay K, van der Molen N, van der Oost R. 2004. Assessment of bioavailable PAH, PCB and OCP concentrations in water, using semipermeable membrane devices (SPMDs), sediments and caged carp. *Chemosphere* 54:1675–1689.
- Petty JD, Jones SB, Huckins JN, Cranor WL, Parris JT, McTague TB, Boyle TP. 2000. An approach for assessment of water quality using semipermeable membrane devices (SPMDs) and bioindicator tests. *Chemosphere* 41:311–321.
- Kansy M, Senner F, Gubernator K. 1998. Physicochemical high throughput screening: Parallel artificial membrane permeation assay in the description of passive absorption processes. *J Med Chem* 41:1007–1010.
- Wohnsland F, Faller B. 2001. High-throughput permeability pH profile and high-throughput alkane/water log P with artificial membranes. *J Med Chem* 44:923–930.
- Zhu C, Jiang L, Chen TM, Hwang KK. 2002. A comparative study of artificial membrane permeability assay for high throughput profiling of drug absorption potential. *Eur J Med Chem* 37:399–407.
- Sugano K, Nabuchi Y, Machida M, Aso Y. 2003. Prediction of human intestinal permeability using artificial membrane permeability. *Int J Pharm* 257:245–251.
- Thompson M, Lennox RB, McClelland RA. 1982. Structure and electrochemical properties of microfiltration filter–lipid membrane systems. *Anal Chem* 54:76–81.
- Henderson JR, Tocher DR. 1987. The lipid composition and biochemistry of freshwater fish. *Prog Lipid Res* 26:281–347.
- Staurnes M, Rainuzzo JR, Sigholt T, Jørgensen L. 1994. Acclimation of Atlantic cod (*Gadus morhua*) to cold water: Stress response, osmoregulation, gill lipid composition and gill Na-K-ATPase activity. *Comp Biochem Physiol A Comp Physiol* 109:413–421.
- Randall DJ, Connell DW, Yang R, Wu SS. 1998. Concentrations of persistent lipophilic compounds in fish are determined by exchange across the gills, not through the food chain. *Chemosphere* 37:1263–1270.
- Könemann H, van Leeuwen K. 1980. Toxicokinetics in fish: Accumulation and elimination of six chlorobenzenes by guppies. *Chemosphere* 9:3–19.
- Banerjee S, Sugatt RH, O'Grady DP. 1984. A simple method for determining bioconcentration parameters of hydrophobic compounds. *Environ Sci Technol* 18:79–81.
- Smith AD, Bharath A, Mallard C, Orr D, McCarty LS, Ozburn GW. 1990. Bioconcentration kinetics of some chlorinated benzenes and chlorinated phenols in American flagfish, *Jordanella floridae*. *Chemosphere* 20:379–386.
- Kalsch W, Nagel R, Urlich K. 1991. Uptake, elimination, and bioconcentration of ten anilines in zebrafish (*Brachydanio rerio*). *Chemosphere* 22:351–363.
- Ensenbach U, Nagel R. 1991. Toxicokinetics of xenobiotics in zebrafish—Comparison between tap and river water. *Comp Biochem Physiol C Comp Pharmacol* 100:49–53.
- Bradbury SP, Dady JM, Fitzsimmons PN, Voit MM, Hammermeister DE, Erickson RJ. 1993. Toxicokinetics and metabolism of aniline and 4-chloroaniline in medaka (*Oryzias latipes*). *Toxicol Appl Pharm* 118:205–214.
- De Wolf W, Yedema ESE, Hermens JLM. 1994. Bioconcentration kinetics of chlorinated anilines in guppy, *Poecilia reticulata*. *Chemosphere* 28:159–167.
- De Wolf W, Mast B, Yedema ESE, Seinen W, Hermens JLM. 1994. Kinetics of 4-chloroanilines in guppy, *Poecilia reticulata*. *Aquat Toxicol* 28:65–78.
- Van Eck JMC, Koelmans AA, Deneer JW. 1997. Uptake and elimination of 1,2,4-trichlorobenzene in the guppy (*Poecilia reticulata*) at sublethal and lethal aqueous concentrations. *Chemosphere* 34:2259–2270.
- De Wolf W, Lieder P. 1998. A novel method to determine uptake and elimination kinetics of volatile chemicals in fish. *Chemosphere* 36:1713–1724.
- Sijm DTHM, Verberne ME, de Jonge WJ, Pärt P, Opperhuizen A. 1995. Allometry in the uptake of hydrophobic chemicals determined in vivo and in isolated perfused gills. *Toxicol Appl Pharm* 131:130–135.
- Avdeef A. 2001. Physicochemical profiling (solubility, permeability and charge state). *Curr Top Med Chem* 1:277–351.
- Gutknecht J, Tosteson DC. 1973. Diffusion of weak acids through lipid bilayer membranes: Effects of chemical reactions in the aqueous unstirred layers. *Science* 182:1258–1261.
- Stumm W, Morgan JJ. 1995. *Aquatic Chemistry—Chemical Equilibria and Rates in Natural Waters*. John Wiley, New York, NY, USA.
- Schwarzenbach RP, Gschwend PM, Imboden DM. 2003. *Environmental Organic Chemistry*, 2nd ed. John Wiley, New York, NY, USA.
- Hawker DW, Connell DW. 1988. Influence of partition coefficient of lipophilic compounds on bioconcentration kinetics with fish. *Water Res* 22:701–707.
- Sijm DTHM, Verberne ME, Pärt P, Opperhuizen A. 1994. Experimentally determined blood and water-flow limitations for uptake of hydrophobic compounds using perfused gills of rainbow trout (*Oncorhynchus mykiss*)—Allometric applications. *Aquat Toxicol* 30:325–341.
- Gaffar MA, Abu El-Fadl A. 1989. Investigation of the pyroelectric and piezoelectric properties of triglycine sulphate single crystals containing organic molecules. *J Phys Condensed Matter* 1:8991–8999.
- U.S. Environmental Protection Agency. 2000. *EPI Suite™*, Ver 3.11. Washington, DC.



## APPENDIX

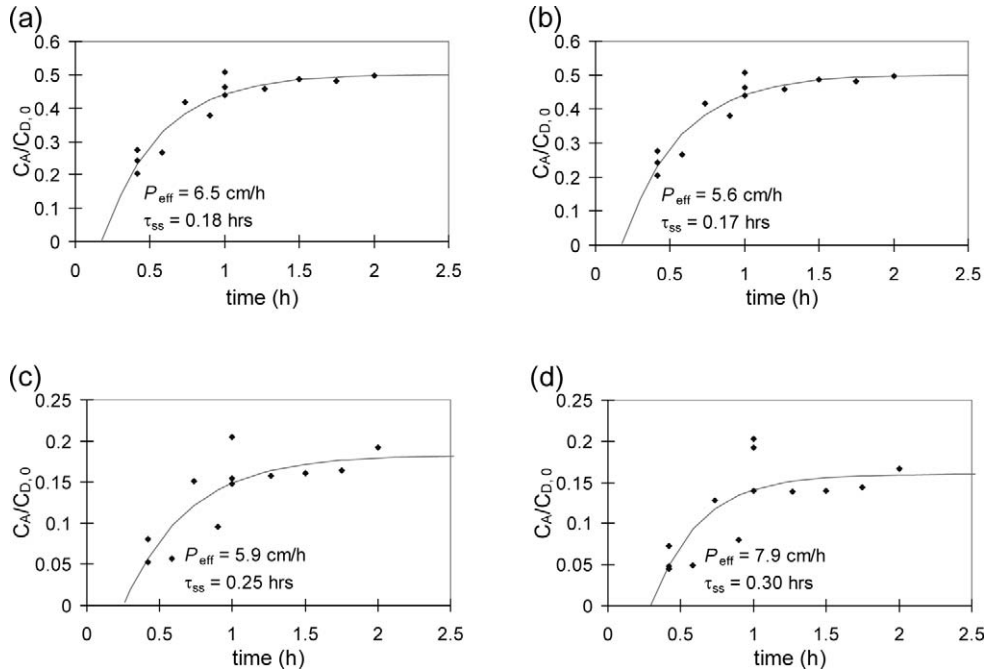


Fig. A1. Determination of the effective membrane permeability by nonlinear regression with Equation 8 for (a) chlorobenzene (CB), (b) bromobenzene (BB), (c) 1,4-dichlorobenzene (14DCB), and (d) 1,3-dichlorobenzene (13DCB).

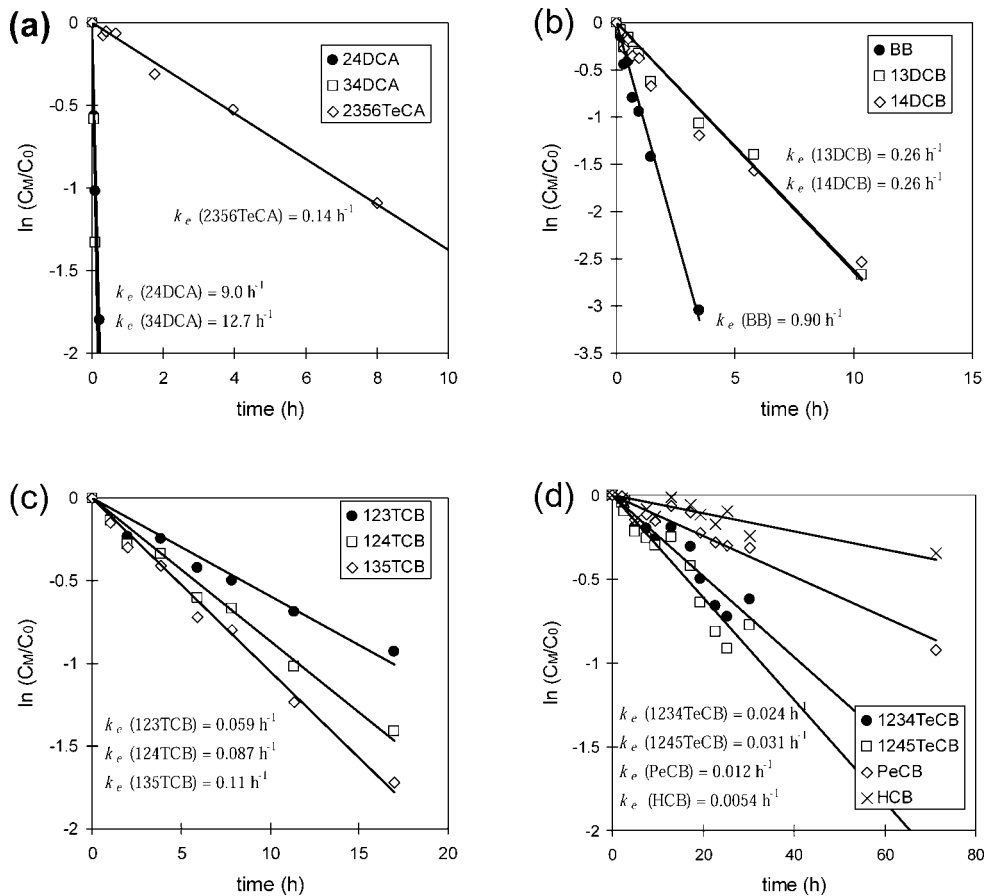


Fig. A2. Determination of first-order elimination rate constant from the artificial membrane system for (a) 2,4-dichloroaniline (24DCA), 3,4-dichloroaniline (34DCA), and 2,3,5,6-tetrachloroaniline (2356TeCA); (b) bromobenzene (BB), 1,3-dichlorobenzene (13DCB), and 1,4-dichlorobenzene (14DCB); (c) 1,2,3-trichlorobenzene (123TCB), 1,2,4-trichlorobenzene (124TCB), and 1,3,5-trichlorobenzene (135TCB); and (d) 1,2,3,4-tetrachlorobenzene (1234TeCB), 1,2,4,5-tetrachlorobenzene (1245TeCB), pentachlorobenzene (PeCB), and hexachlorobenzene (HCB).

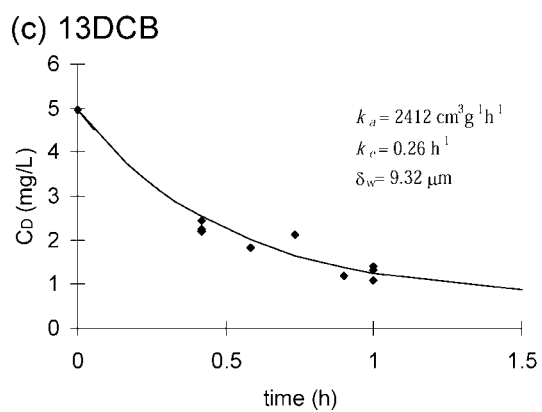
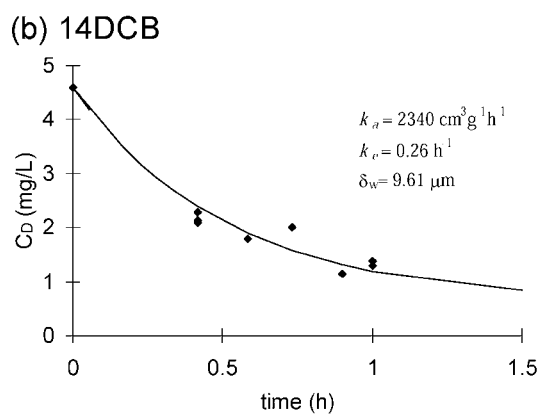
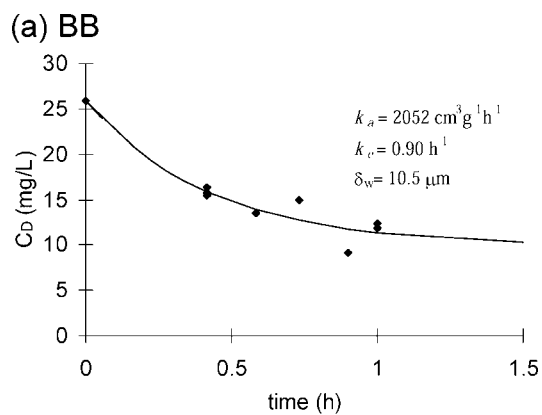


Fig. A3. Estimation of the donor side thickness of the diffusion film. Best fit parameter,  $k_a$ , was obtained from measured elimination rate constants.  $\delta_w$  was calculated from Equation 2 assuming that this process is solely limited by aqueous diffusion.